OPEN ACCESS
International Journal of Computational Materials
Science and Engineering
Vol. 11, No. 3 (2022) 2250003 (25 pages)

DOI: 10.1142/S2047684122500038

A fractional approach to fluid flow and solute transport within deformable saturated porous media

Valentina A. Salomoni*
Department of Management and Engineering
University of Padua, Stradella S. Nicola 3, 36100 Vicenza, Italy
valentina.salomoni@unipd.it

Nico De Marchi
Department of Civil, Environmental and Architectural Engineering
University of Padua, Via F. Marzolo 9, 35131 Padua, Italy
nico.demarchi@unipd.it

Received 8 December 2021
Revised 5 February 2022
Accepted 6 February 2022
Published 15 March 2022

The non-Darcian flow and solute transport in geometrically nonlinear porous media are modeled with Riesz derivative solved via Simpson's rule or treated through the Grünwald–Letnikow definition and subsequently discretized via Finite Difference schemes when considering anomalous diffusion, nonlinear diffusion, or anomalous solute advection–dispersion, respectively. Particularly, the standard diffusion and advection–dispersion equations are converted into fractional equations to take into account memory effects as well as non-Fickian dispersion processes. Hence, a 3D hydro-mechanical model accounting for geometric nonlinearities is correspondingly developed including the fractional diffusion–advection–dispersion equations (FRADEs) and a series of one-dimensional analyses are performed with validation purposes.

Keywords: Fractional derivative; fractional diffusion equation; fractional advection–dispersion equation; solute transport; porous media; finite strain.

1. Introduction

Solutes are materials that dissolve in liquids forming solutions, e.g., salt (not at very large concentrations) in water (the solvent). The transport of a solute within porous media depends on several factors, including solvent and solute properties, fluid velocity field within the porous medium, and microgeometry, i.e., shape, size, and location of the solid part of the medium and the void [Goldsztein, 2008].

*Corresponding author.

Solute transport in liquid-filled porous media plays a significant role in several phenomena including the transport of contaminants in soils [e.g., Brusseau, 1994; Elfeki *et al.*, 1997; Zhang *et al.*, 2013; Zou *et al.*, 2017], transport of nutrients in bones [Blair *et al.*, 2007; Knothe Tate and Knothe, 2000; Wang, 2018], the intrusion of radioactive wastes within cemented materials [Majorana and Salomoni, 2004], secondary recovery techniques in oil reservoirs (where the injected fluid dissolves the reservoir's oil), the use of tracers in petroleum engineering and hydrology research projects [Lewis and Schrefler, 1998; Schrefler *et al.*, 1999], etc.

Modeling coupled moisture flows within deformable saturated/partially saturated porous media is a widely investigated field since the pioneer works by Biot [1941, 1956] for establishing complete theoretical frameworks able to represent multi-component systems in isothermal and nonisothermal conditions [e.g., Lewis and Schrefler, 1998; Borja, 2004; Coussy, 2004; de Boer, 2005; Zhang *et al.*, 2013].

In any case, several field experiments for the solute transport in highly heterogeneous media [e.g., Schumer *et al.*, 2003; Zhang *et al.*, 2009; Fomin *et al.*, 2010] demonstrate that solute concentration profiles exhibit anomalous non-Fickian growth rates and so-called "heavy tails", the effects which cannot be predicted via the standard mass transport equation [Fomin *et al.*, 2011] but via fractional-order differential equations that may be viewed as long-time and long-space limits of continuous-time random walk (CTRW) [Neretnieks, 1980; Hilfer and Anton, 1995; Barkai *et al.*, 2000; Metzler and Compte, 2000; Meerschaert *et al.*, 2002; Deng *et al.*, 2004, 2006]]; correspondingly, the Fickian advection–dispersion equation (ADE), unable to reflect the long-tail dispersion process, is converted into a fractional diffusion–advection–dispersion equation (FRADE). The FRADE approach appears to have the potential for the prediction of non-Fickian dispersion processes, but its wide application is hindered by the difficulty of obtaining analytical solutions, especially when reaction terms are incorporated [Deng *et al.*, 2004]. Alternatively, nonlocal problems accounting for long-range interactions can be treated via nonlocal integral models [Pinnola *et al.*, 2021] and even combined time-fractional and space-nonlocal strategies [Barretta *et al.*, 2021].

Additionally, when considering water flow in low-permeability porous media, a nonlinear relationship between water flux and hydraulic gradient should be considered, thereby indicating a non-Darcian flow; hence, for developing a more appropriate description able to include a memory effect, the existing relationships can be modified in a fractional fashion [Zhou *et al.*, 2019].

In this work, a coupled three-dimensional fractional hydro-mechanical model in finite strains [Borja, 2013] based on the modified mixture theory [Borja and Alarcón, 1995; Pomaro *et al.*, 2011; Sun, 2015] is developed from previous versions for saturated porous media [Spiezia *et al.*, 2016; Salomoni, 2018; De Marchi *et al.*, 2019]. Particularly, the upgraded model includes solute transport, but more importantly, the constitutive equation for pore fluid is converted first into a linear fractional one to account for anomalous diffusion by computing the integral version of the half-Laplacian via Simpson's rule, then into a nonlinear fractional one (obtaining the

porous medium equation) solved via a Finite Difference scheme in one-dimensional domains. Correspondingly, also the advection–dispersion equation for solute flux is transformed into a fractional one (FRADE) with the Riesz derivative treated through the Grünwald definition which appears convenient for numerical solutions. Particularly, a series of 1D Finite Difference analyses have been developed adopting the fractional-centered derivative scheme [Owolabi and Atangana, 2019] combined with the β-method, with the advective term treated via the Lax–Wendroff scheme. In the most general case of advection–dispersion phenomena including overpressure effects, the numerical algorithm has been enriched following the lines described by Deng *et al.* [2004] based on the split-operator method; hence, the advection step has been solved via an explicit second-order midpoint method, together with the β-method for the fractional diffusion/dispersion step and the trapezoidal rule for the fluid excess step.

2. Governing Equations

The main hydro-mechanical equations are briefly recalled in the following, concentrating on the upgrades from the model already described in Salomoni [2018].

2.1. *Balance and constitutive equations for the solid skeleton*

The balance of linear momentum for a saturated porous medium can be written as, assuming incompressibility of the solid and liquid phases,

$$\rho \mathbf{g} + \nabla \cdot \boldsymbol{\sigma} = \mathbf{0}, \tag{2.1}$$

where $\rho = \rho_s\ (1 - \varphi) + \rho_w \varphi$ is the saturated mass density of the solid–fluid mixture (φ being the porosity) and σ the Cauchy total stress tensor, with

$$\boldsymbol{\sigma} = \boldsymbol{\sigma'} - p\mathbf{I}, \tag{2.2}$$

where σ' is the effective stress and p is pore pressure (with the drained bulk modulus of the solid grain being much higher than that of the skeleton).

In the total Lagrangian formulation, Eq. (2.1) is rewritten in the reference configuration (X) via the Piola transformation, i.e.,

$$J\rho \mathbf{G} + \nabla_X \cdot \mathbf{P} = \mathbf{0}, \tag{2.3}$$

where $\mathbf{P}$ is the total first Piola–Kirchhoff stress tensor obtained from pull-back of $\boldsymbol{\sigma}$,

$$\mathbf{P} = J\boldsymbol{\sigma} \cdot \mathbf{F}^{-T}, \tag{2.4}$$

and $J = \det(\mathbf{F}) > 0$, with $\mathbf{F}(\mathbf{X}, t)$ being the deformation gradient of the solid skeleton [Simo and Hughes, 1998; Holzapfel, 2000; Majorana *et al.*, 2010],

$$\mathbf{F} = \frac{\partial \varphi(\mathbf{X}, t)}{\partial \mathbf{X}}, \tag{2.5}$$

with $\varphi(\mathbf{X}, t)$ being the (local) motion.

We assume to refer to the Hencky strain tensor $\mathbf{h}$, typical for characterizing finite isotropic hyperelasticity, as a measure of deformation [Karrech *et al.*, 2011]

$$\mathbf{h} = \frac{1}{2} \ln \mathbf{b}, \tag{2.6}$$

in which $\mathbf{b}$ is the left Cauchy–Green strain tensor, $\mathbf{b} = \mathbf{F} \cdot \mathbf{F}^T$, and, developing the spectral decomposition,

$$\mathbf{h} = \frac{1}{2} \sum_{A=1}^{3} \ln \lambda_A \mathbf{n}_A \otimes \mathbf{n}_A, \tag{2.7}$$

with λ_A and $\mathbf{n}_A$ being the eigenvalues and eigenvectors of $\mathbf{b}$, respectively.

Correspondingly, the incremental stress–strain relationship can be written as [Karrech *et al.*, 2012]

$$d\sigma = \left(\kappa - \frac{2}{3} G \right) \frac{1 - \vartheta}{J} d\vartheta \mathbf{I} + 2G \frac{1 - \vartheta}{J} d\mathbf{h} - dp_w \mathbf{I}, \quad d\vartheta = \mathrm{tr} d\mathbf{h}, \tag{2.8}$$

with G being the shear modulus of the porous material.

2.2. *Balance and constitutive equations for pore fluid*

The local fluid content continuity equation in isothermal conditions can be written as

$$\nabla \cdot \mathbf{v} - \frac{1}{\rho_w} \nabla \cdot \left(\rho_w \frac{\mathbf{k}}{\mu} \cdot (\nabla p - \rho_w \mathbf{g}) \right) = \mathbf{0}. \tag{2.9}$$

2.3. *Balance equations for solute transport*

By extending the one-dimensional approach of Zhang *et al.* [2013] to three-dimensional domains, the mass conservation equation for the solute in the solid phase can be written as

$$\frac{D}{Dt}[(1 - \varphi) \rho_s m_s J] = \dot{M}_{a \to s}, \tag{2.10}$$

where m_s is the mass of solute sorbed on or within the solid phase per unit mass of the solid phase and $\dot{M}_{a \to s}$ denotes the rate of solute loss in the water phase by solid-phase sorption; hence, considering the stationarity of the solid content, Eq. (2.10) reduces to

$$(1 - \varphi) \rho_s J \dot{m}_s = \dot{M}_{a \to s}. \tag{2.11}$$

The mass conservation equation for solute in the fluid phase is

$$\frac{D}{Dt}[\varphi C J] = -\nabla \cdot \mathbf{q}_f - \dot{M}_{a \to s}, \tag{2.12}$$

where C is the concentration of the solute in the pore fluid and $\mathbf{q}_f$ represents the solute flux in the fluid phase, leading to

$$\dot{J}C + J(\varphi - 1)\dot{C} = -\nabla \cdot \mathbf{q}_f - \dot{M}_{a\to s}, \tag{2.13}$$

and, extending the expression of $\mathbf{q}_f$ according to [Peters and Smith, 2002]

$$\mathbf{q}_f = \varphi \mathbf{w} C - \frac{\varphi \mathbf{D}}{J} \cdot \nabla C, \tag{2.14}$$

in which $\mathbf{D}$ is the hydrodynamic dispersion tensor, given by the sum of the effective diffusion $\mathbf{D}_e$ and the mechanical dispersion tensor $\mathbf{D}_m$. However, in case of fine-grained soils where Darcy velocity is low (approximately around 10^{-6} m/s), the mechanical dispersion values can be expected to be relatively small [Lewis *et al.*, 2009]. Hence, the combined solute transport within the matrix–fluid system can be written as

$$(1-\varphi)J\dot{C}(\rho_s K_d - 1) + J\dot{C}\nabla \cdot \mathbf{v} = -\nabla \cdot \left[\varphi \rho_w C \left(\frac{\mathbf{k}}{\mu} \cdot (\nabla p - \rho_w \mathbf{g})\right)\right] + \nabla \cdot \left(\frac{\varphi \mathbf{D}}{J} \cdot \nabla C\right). \tag{2.15}$$

In Eq. (2.15), it has been considered to neglect the effect of sorption (being medium in saturated conditions), so that the concentration of solute in the solid phase can be assumed to be linearly dependent on the concentration of the solute in the pore fluid via the contaminant partitioning coefficient K_d [Mathur and Jayawardena, 2008].

2.3.1. *Fractional dispersion approach to solute flux*

It is to be noticed that the second term on the RHS of Eq. (2.14) assumes that mass transport media are isotropic [Fischer *et al.*, 1979; Deng *et al.*, 2006], which is rarely the case. Hence, the approach by Chaves [1998], Meerschaert *et al.* [1999], and particularly Deng *et al.* [2006], proposing a general flux law of molecular diffusion based on the revision of Fick's diffusion law, has been followed.

According to this approach, the stated term of the solute flux is decomposed into a solute flux produced by molecular diffusion, a solute flux produced by turbulent diffusion, plus a solute flux produced by shear flow dispersion; in any case, it has been found that the first two contributions, expressed as a linear combination of the Riemann–Liouville operator and the Weyl fractional derivative [Benson *et al.*, 2000; Schumer *et al.*, 2001], are much smaller than the third [McCutcheon, 1989]. By assuming that the dispersion contribution represented by the Riemann–Liouville derivative prevails on the molecular diffusion one, the second RHS term of Eq. (2.14) becomes

$$\mathbf{q}_\alpha = -\frac{\varphi \mathbf{D}}{J} \cdot \nabla^{\alpha-1} C, \tag{2.16}$$

where α is a fractional differential order [Deng *et al.*, 2004] so that, choosing the Grünwald definition for fractional derivative which appears convenient for numerical solutions [Oldham and Spanier, 1974], the value of a fractional differential operator acting on the generic 3D function $\Psi(x_i,t)$ becomes an infinite series, i.e.,

$$\frac{\partial^\alpha \Psi(x_i,t)}{\partial x_i^\alpha} = \lim_{N_i\to\infty} \frac{1}{h_i^\alpha \Gamma(-\alpha)} \sum_{j=0}^{N_i-1} \frac{\Gamma(j-\alpha)}{\Gamma(j+1)} \Psi\Big(x_i + \frac{\alpha}{2}h_i - jh_i, t\Big), \quad (2.17)$$

in which $i = (x, y, z)$, $h_i = \Delta x_i = x_i/N_i$, where N_i is a positive integer, and $\Gamma(\cdot)$ is the gamma function.

Equation (2.15) can be rewritten as

$$(1-\varphi)J\dot{C}(\rho_s K_d - 1) + JC\nabla\cdot\mathbf{v} = -\nabla\cdot\left[\varphi\rho_w C\left(\frac{\mathbf{k}}{\mu}\cdot(\nabla p - \rho_w\mathbf{g})\right)\right] + \nabla\cdot\left(\frac{\varphi\mathbf{D}}{J}\right) \cdot\nabla^{\alpha-1}C + \frac{\varphi\mathbf{D}}{J}\cdot\nabla^\alpha C. \quad (2.18)$$

As extensively described by Deng *et al.* [2006], the fractor α physically reflects the heterogeneity of the soil medium in which the solute is transported and for isotropic media, $\alpha = 2$; the more heterogeneous the medium is, the smaller the α is than the integer constant of 2. Its decrease reproduces an increase in the resistance of the medium to solute dispersion and transport, so leading to delay the phenomenon.

2.4. *Balance equations accounting for anomalous water diffusion and solute dispersion*

It is to be underlined that even the Darcy's law in itself can be treated in a fractional fashion if an anomalous diffusive phenomenon is additionally associated to the transport fluid to take into account the observed memory effects [Vazquez, 2017], having been proved that assuming a temporal variation of permeability is equivalent to considering a dependence of the flux on the fractional derivative of pressure; particularly, the effect of fluid pressure at the boundary on the flow in the porous medium is delayed and the flow occurs as if the medium had a memory [Caputo, 2000; El-Amin *et al.*, 2017]. Some data on the flow of fluids in rocks and porous media show in fact that some fluids can carry solid particles that may obstruct some of the pores, or some may precipitate minerals in the pores diminishing their size or even closing them in geothermal areas.

Hence, the complete system of fractional transport equations for pore fluid and solute is given by

$$\rho_w\nabla\cdot\mathbf{v} - \nabla\cdot\left(\rho_w\frac{\mathbf{k}}{\mu}\cdot(\nabla^{\alpha-1}p - \rho_w\mathbf{g})\right) = 0, \quad (2.19)$$

together with Eq. (2.18).

3. One-Dimensional Consolidation with Fractional-Space Diffusion–Advection–Dispersion Equations

3.1. *Solution of the fractional transport equation for pore fluid (FRDE): Linear case*

When considering 1D consolidation [Peters and Smith, 2002; Lewis *et al.*, 2009; Zhang *et al.*, 2013; Zou *et al.*, 2017], or a 1D fluid-injection source in a borehole [Carcione and Gei, 2009] with negligible self-weight, no changes in vertical stress, and permeability independent of deformation, the model can be simplified as follows.

Under these assumptions, the logarithmic strain can be written as

$$\vartheta \approx \frac{p - p_0 + \sigma - \sigma_0}{\kappa + \frac{4}{3}G}, \tag{3.1}$$

with p_0 and σ_0 being the initial values of pore pressure and axial stress, respectively. Correspondingly, the FRDE for pore fluid (2.19) becomes, by assuming space independence of density, $\rho_w = \rho_0$,

$$\frac{1}{\kappa + \frac{4}{3}G}\left(\frac{\partial p}{\partial t} + \frac{\partial \sigma}{\partial t}\right) - \frac{k}{\mu}(-\Delta)^{\frac{\alpha}{2}} p = 0. \tag{3.2}$$

In case σ_0 is instantaneously applied, Eq. (3.2) reduces to

$$\frac{1}{\kappa + \frac{4}{3}G}\frac{\partial p}{\partial t} - \frac{k}{\mu}(-\Delta)^{\frac{\alpha}{2}} p = 0. \tag{3.3}$$

In the form of Eq. (3.3), the balance of fluid content does not include advection and this situation is analogous to the one accounting for sub-critical drifts when diffusion dominates, so that (3.3) is similar to the fractional parabolic heat equation [Vazquez, 2017; Greco and Iannizzotto, 2017; Delgadino and Smith, 2018] and $(-\Delta)^{\beta}$ can be seen as a fractional power of the Laplacian operator through Riesz potential [notice that the expression is an alternative representation to Eq. (2.17)],

$$(-\Delta)^{\beta} u(x) = C_{N,\beta}\mathrm{PV}\int_{\Re^N} \frac{u(x) - u(y)}{|x - y|^{N+2\beta}} dx, \quad \beta \in (0,1), \ \ N \geq 1, \tag{3.4}$$

where $u : \Re^N \to \Re$, PV stands for "principal value", and $C_{N,\beta} > 0$ is a suitable normalizing constant [Greco and Iannizzotto, 2017]. The outstanding feature of $(-\Delta)^{\beta}$ is *nonlocality*, i.e., the quantity $(-\Delta)^{\beta} u(x)$ depends not only on the values of u in a neighborhood of x (as in the case of the standard Laplacian), but rather on the values of u at any point $y \in \Re^N$. In the limit $\beta \to 1$ (i.e., $\alpha \to 2$), the standard Laplace operator is recovered, but there is a big difference between the local operator $(-\Delta)$ that appears in the classical heat equation and represents Brownian motion, and the nonlocal family $(-\Delta)^{\beta}$, $0 < \beta < 1$. The latter are generators of Levy processes that include jumps and long-distance interactions, resulting in *anomalous diffusion* [Vazquez, 2017].

It is to be underlined that in Eq. (3.2) the fluid pressure is coupled with the strain via Eq. (3.1), which makes the problem more difficult to solve, but there are situations in which these field variables can be uncoupled, e.g., when the displacement field is irrotational or when the fluid is very compressible [Detournay and Cheng, 1993]. In any case, Carcione and Gei [2009] showed that it is possible to use a less stringent approximation when considering the fluid-injection source in a borehole, transverse isotropy of the elastic and transport properties, uniaxial strain conditions, and vertical deformation only, together with no changes in the vertical stress. Under these conditions, they obtained the same expression as of Eq. (3.2) (with $\beta = 1$, and the approach used there not being fractional), with $\partial\sigma/\partial t$ considered as a source term.

Hence, in compact form the FRDE becomes

$$\frac{\partial p}{\partial t} = K_0(-\Delta)^{\frac{\alpha}{2}} p, \tag{3.5}$$

where $K_0 = \frac{k}{\mu}(\kappa + \frac{4}{3}G)$ is the equivalent diffusion coefficient; for simplicity, $K_0 = 1$ can be assumed in all calculations [Tasbozan *et al.*, 2013].

The solution of the standard (nonfractional) diffusion equation (DE) for an infinitely long straight line gives, via Fourier transform [Merryfield, 2009; Vazquez, 2017],

$$p(x,t) = \frac{1}{\sqrt{4\pi t}} \int f(y) e^{-\frac{(x-y)^2}{4t}} dy, \quad p(x,0) = f(x), \tag{3.6}$$

and

$$G(x,t) = \frac{1}{\sqrt{4\pi t}} e^{-\frac{|x|^2}{4t}} \tag{3.7}$$

is the Gaussian function, working as a kernel.

Similarly, by applying Fourier transform to the FRDE (3.5) and subsequently the inverse transform [Vazquez, 2018], the fractional diffusion equation can be solved for all $0 < \alpha/2 \leq 1$ by means of the *fundamental solution*, $P(x,t;\alpha)$,

$$p(x,t) = \int f(y) P(x-y,t;\alpha) dy. \tag{3.8}$$

The kernel

$$P(x,t;\alpha) = C_{N,\alpha} \frac{t}{(t^{\frac{2}{\alpha}} + |x|^2)^{\frac{1+\alpha}{2}}}, \tag{3.9}$$

with $C_{N,\alpha} = C_{1,\alpha} = \Gamma(\frac{2+\alpha}{2})/\pi^{\frac{2+\alpha}{2}}$ being explicit only for $\alpha = 1$; when $\alpha = 2$, the Gaussian kernel (3.7) for the standard heat equation holds; note the marked difference with the Gaussian kernel: the behavior as x goes to infinity of the function $P(x,t;\alpha)$ is power-like (with a so-called *fat tail*) while $G(x,t)$ has an exponential spatial decay. This difference is expected in a theory of long-distance interactions. The graphical representations of the (normalized) kernels $G(x,t)$ and $P(x,t;1)$ are shown in Fig. 1 in the dimensionless time–space domain.

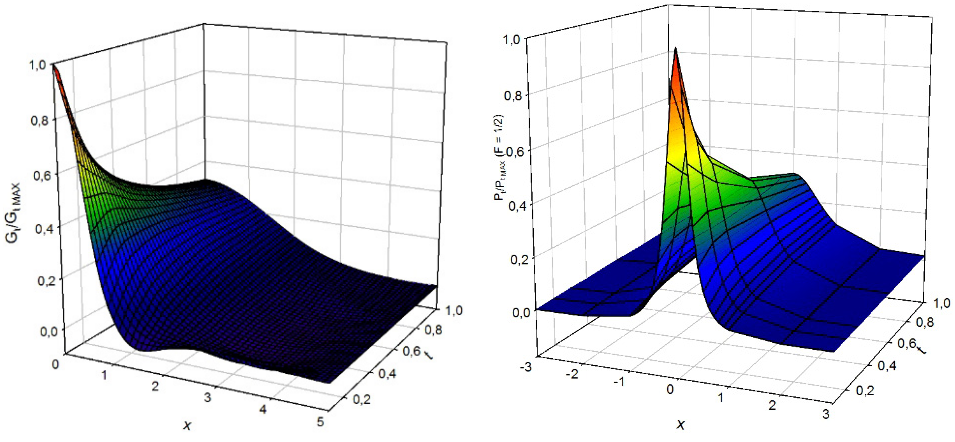

(a) (b)

Fig. 1. Normalized kernels for standard DE: (a) half-space and (b) FRDE.

The solution of Eq. (3.6) can be obtained via Fourier series [Salomoni, 2018] or numerical integration (e.g., by adopting Simpson's rule), whereas Eq. (3.8), with $\alpha = 1$, requires numerical integration, so the latter strategy has been used here for reaching both solutions

$$p(x,t) = \frac{1}{\sqrt{4\pi t}}\bar{A}(x) \quad p_\alpha(x,t) = C_{N,1}\bar{B}(x), \tag{3.10}$$

where $p_\alpha(x,t)$ refers to the anomalous diffusion solution and

$$\bar{A}(x) \cong \frac{\Delta y}{\zeta}\sum_{\zeta}^{\bar{A}}(x) \quad \bar{B}(x) \cong \frac{\Delta y}{\zeta}\sum_{\zeta}^{\bar{B}}(x). \tag{3.11}$$

When performing Simpson's rule $\zeta = 3$, so that

$$\begin{aligned}\sum_{3}^{\bar{A}}(x) &= \sum_{3}^{\bar{A}}(x-2\Delta y) + [f(x-2\Delta y)G'(x-2\Delta y,t) + 4f(x-\Delta y)G'(x-\Delta y,t)\\ &\quad + f(x)G'(x,t)],\\ \sum_{\zeta}^{\bar{B}}(x) &= \sum_{\zeta}^{\bar{B}}(x-2\Delta y) + [f(x-2\Delta y)P'(x-2\Delta y,t) + 4f(x-\Delta y)P'(x-\Delta y,t)\\ &\quad + f(x)P'(x,t)],\end{aligned} \tag{3.12}$$

with

$$G'(x,t) = e^{-\frac{|x|^2}{4t}}, \quad P'(x,t) = \frac{t}{(t^2+|x|^2)}, \tag{3.13}$$

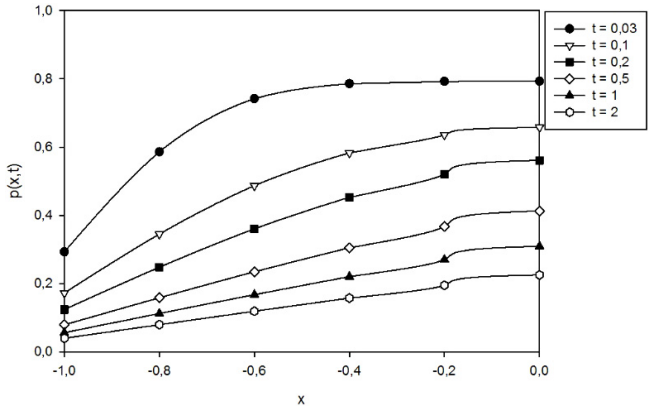

Fig. 2. Spatial pressure profiles from a standard diffusion problem.

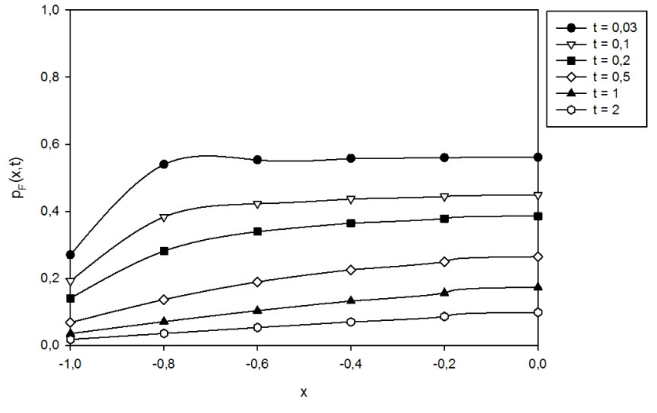

Fig. 3. Spatial pressure profiles from a fractional diffusion problem.

and assuming

$$p(x,0) = f(x) = \begin{cases} 1 & \text{for } -1 \le x \le 1 \\ 0 & \text{otherwise} \end{cases}. \tag{3.14}$$

The dimensionless pressures versus the dimensionless half-space resulting from the DE and the FRDE, respectively, are plotted in Figs. 2 and 3 at variables times.

By examining these figures, together with Fig. 4, it can be observed that the nonlocality of the fractional Laplacian affects the solution, influencing both the shape and the global diffusion velocity; in fact, the predicted fractional diffusion gradients are lower than those for standard diffusion all along the bar (but mainly at the bar's edge) independently of time, with the diffusion process appearing to be delayed (with lower velocities at the beginning of the process, approaching equal values at higher times).

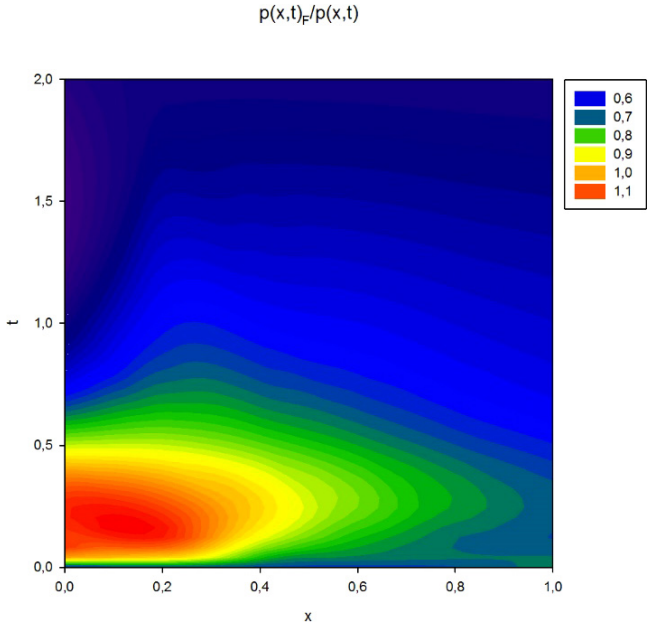

Fig. 4. Space–time distribution of fractional/nonfractional solution ratio.

In fact, physically the fractional term is used to describe the long-tailed diffusion problem caused by surface and volume heterogeneities of the solid media.

3.2. *Solution of the fractional transport equation for pore fluid: Nonlinear case*

The previous solution is valid, as stated, particularly when a constant permeability is assumed throughout the domain; hence, we can observe that, for variable permeability, Eq. (2.9) becomes [after introducing Eq. (3.1)]

$$\frac{\partial p}{\partial t} = \left(\kappa + \frac{4}{3}G\right) \nabla \cdot \left(\frac{k}{\mu} \cdot (\nabla p - \rho_w g)\right), \tag{3.15}$$

therefore resulting in the Porous Medium Equation (PME) [Nguyen and Vazquez, 2018], with a forcing term, representing a *degenerate parabolic equation*. Apart from a constant, the diffusion coefficient takes the expression

$$D(p) = \frac{k}{\mu} = |p|^{m-1}, \quad m > 1, \tag{3.16}$$

in which the standard diffusion equation can be considered as the limit of the PME when $m \to 1$.

With fractional diffusion, Eq. (3.15) takes the form [de Pablo *et al.*, 2011] of

$$\frac{\partial p}{\partial t} = (-\Delta)^{1/2}(|p|^{m-1}p). \tag{3.17}$$

Equations of the type of (3.17) can be considered as nonlinear variations of the linear fractional diffusion equation previously studied (i.e., *anomalous diffusion*). Equation (3.17), together with the initial conditions as of (3.14) and $m > m_c = \max\{(N-2s)/N, 0\}$, has been proved [Stan *et al.*, 2019] to admit a unique fundamental solution [we recall that once the fundamental solution is found, the desired solution of the original equation can be achieved by convolution, see, e.g., Eq. (2.10)] with the self-similar (*Barenblatt*) form

$$p_M^*(x,t) = t^{-\chi} f(|x|t^{-\delta}), \tag{3.18}$$

with

$$\chi = \frac{N}{N(m-1)+2s}, \quad \delta = \frac{1}{N(m-1)+2s}. \tag{3.19}$$

In our case $N = 1$ and $s = 1/2$, and the computed normalized Barenblatt profiles in the dimensionless time–space domain, for $m = 2$ and $m = 10$, are reported in Fig. 5; notice that, for $m = 1$ (linear case), the kernel coincides with that for anomalous diffusion [Vazquez, 2014] and when $m = 1$ together with $s = 1$, the Gaussian heat kernel is obtained.

In the case of nonlinear fractional diffusion, it is still an open question to find explicit or semi-explicit solutions for the problem (3.17) [Stan *et al.*, 2019], with an integral representation of the evolution like (3.8) being not available [Vazquez, 2014], hence an approach via Finite Differences similar to the one in del Teso [2014] must be followed.

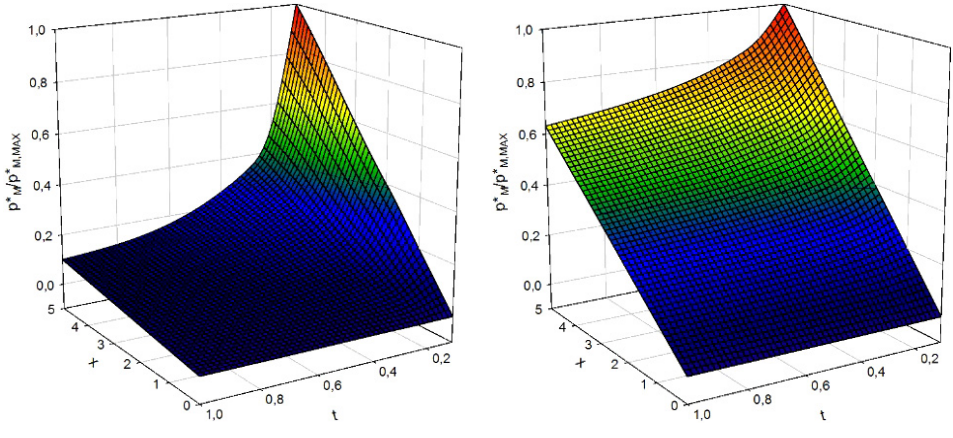

(a) (b)

Fig. 5. Computed Barenblatt profiles for (a) $m = 2$ and (b) $m = 10$ with $s = 1/2$.

Particularly, it has been chosen here to adopt the fractional-centered derivative scheme [Owolabi and Atangana, 2019] combined with the β-method. Different choices of the β-parameter allow us to obtain three different time integration schemes: with $\beta = 0$, the conditionally stable Forward Euler scheme is obtained, and with $\beta = 1, 1/2$ the implicit Backward Euler and the Crank–Nicolson schemes, respectively.

3.3. *General 1D solution in case of anomalous solute diffusion*

The system of FRADE (2.18)–(2.19) is partly uncoupled due to the independence of the transport equation for pore fluid from solute concentration, so that the pressure values can be treated as known data within Eq. (2.18). By introducing Eq. (2.19) into Eq. (2.18) and neglecting spatial nonlinear effects for fluid properties, the 1D saturated model in finite strains is governed by

$$(1-\varphi)J(\rho_s K_d - 1)\dot{C} + \left(\varphi\rho_w \frac{k}{\mu}\frac{\partial p}{\partial x}\right)\frac{\partial C}{\partial x} + (J + \varphi\rho_w)\frac{k}{\mu}\frac{\partial^2 p}{\partial x^2}C - \frac{\varphi D}{J}\cdot(-\Delta)^{\frac{\alpha}{2}}C = 0. \tag{3.20}$$

Similar observations can be done for the Jacobian, which introduces an additional coupling with the mechanical part; in fact, recalling that $\vartheta = \ln J$, the Jacobian appears to be directly related to pore pressure [see Eq. (3.1)], so that it also can be treated as a known term.

For the sake of simplicity, the nonlocality feature of Eq. (3.20) is now attributed to the solute only; in any case, with the pore fluid distribution being reachable independently on (3.20), some nonlocality related to pore pressure can be regardless introduced by taking the results of Sec. 3.1 or 3.2.

Equation (3.20) involves effectively three processes of solute transport: the second term denotes advection caused by fluid flow, the third term reflects the transfer of solute resulting from pore fluid excess, and the fractional-order derivative term represents the contribution of dispersion in a heterogeneous medium.

To avoid the use of uncertain initial concentrations, the above equation can be transformed into a transport rate equation; hence, replacing C by CQ_f/Q_f, with Q_f being the flow discharge,

$$\begin{aligned}(1-\varphi)J(\rho_s K_d - 1)\frac{\partial \bar{C}}{\partial t} + \left(\varphi\rho_w \frac{k}{\mu}\frac{\partial p}{\partial x}\right)\frac{\partial \bar{C}}{\partial x} + Q_f\Bigg[(1-\varphi)J(\rho_s K_d - 1)\frac{\partial(1/Q_f)}{\partial t} \\ + \left(\varphi\rho_w \frac{k}{\mu}\frac{\partial p}{\partial x}\right)\frac{\partial(1/Q_f)}{\partial x} - \frac{\varphi D}{J}\cdot(-\Delta)^{\frac{\alpha}{2}}(1/Q_f)\Bigg]\bar{C} + (J + \varphi\rho_w)\frac{k}{\mu} \\ \times \frac{\partial^2 p}{\partial x^2}\bar{C} - \frac{\varphi D}{J}\cdot(-\Delta)^{\frac{\alpha}{2}}\bar{C} = 0,\end{aligned} \tag{3.21}$$

with $\bar{C} = CQ_f$ being termed as the transport rate of solute in the flow. With the position

$$\bar{Q}_f = Q_f \left[(1-\varphi) J(\rho_s K_d - 1) \frac{\partial (1/Q_f)}{\partial t} + \left(\varphi \rho_w \frac{k}{\mu} \frac{\partial p}{\partial x} \right) \frac{\partial (1/Q_f)}{\partial x} - \frac{\varphi D}{J} \cdot (-\Delta)^{\frac{\alpha}{2}} (1/Q_f) \right], \tag{3.22}$$

Eq. (3.21) becomes

$$(1-\varphi) J(\rho_s K_d - 1) \frac{\partial \bar{C}}{\partial t} + \left(\varphi \rho_w \frac{k}{\mu} \frac{\partial p}{\partial x} \right) \frac{\partial \bar{C}}{\partial x} + \left[\bar{Q}_f + (J + \varphi \rho_w) \frac{k}{\mu} \frac{\partial^2 p}{\partial x^2} \right] \bar{C} - \frac{\varphi D}{J} \cdot (-\Delta)^{\frac{\alpha}{2}} \bar{C} = 0, \tag{3.23}$$

which can be rewritten as

$$\frac{\partial \bar{C}}{\partial t} + \bar{u} \frac{\partial \bar{C}}{\partial x} + \bar{Y} \bar{C} - \bar{K} \cdot (-\Delta)^{\frac{\alpha}{2}} \bar{C} = 0, \tag{3.24}$$

with

$$\bar{u} = \frac{\varphi \rho_w k}{(1-\varphi) J (\rho_s K_d - 1) \mu} \frac{\partial p}{\partial x}, \quad \bar{Y} = \frac{\bar{Q}_f + (J + \varphi \rho_w) \frac{k}{\mu} \frac{\partial^2 p}{\partial x^2}}{(1-\varphi) J (\rho_s K_d - 1)}, \quad \bar{K} = \frac{\varphi D}{J^2 (1-\varphi)(\rho_s K_d - 1)}. \tag{3.25}$$

3.3.1. *Solution of FRDE*

The dispersion process in Eq. (3.24) can be simulated by the sub-equation [having clearly the same structure as of Eqs. (3.5) and (3.17)]

$$\frac{\partial C}{\partial t} = \bar{K} \cdot (-\Delta)^{\frac{\alpha}{2}} C + f \tag{3.26}$$

(where it has been assumed for simplicity $\bar{C} = C$), with f being the forcing function; while the boundary and initial conditions are given by

$$\begin{aligned} &C(x,0) = C^i(x,0), \qquad x \in [a,b]. \\ &C(a,t) = C(b,t) = 0, \quad t > 0. \end{aligned} \tag{3.27}$$

By treating the fractional operator via the Riesz approach and developing the β-method, we have

$$\dot{C}^{t+\beta} = (1-\beta) C^t + \beta C^{t+1} \quad \text{with } \dot{C}^t = \frac{C^{t+1} - C^t}{\Delta t}, \tag{3.28}$$

obtaining the system

$$(\mathbf{I} - \beta \mathbf{B}) C^{t+1} = [\mathbf{I} + (1-\beta)\mathbf{B}] C^t + (\mathbf{F}^t + \beta \Delta \mathbf{F}) \Delta t, \tag{3.29}$$

with $\mathbf{I}$ being the identity and $\mathbf{B}$ the diffusivity matrix, respectively,

$$\mathbf{B} = \bar{K}\frac{\Delta t}{\Delta x^{\alpha}}\begin{bmatrix} p_0 & p_1 & p_2 & \dots & 0 \\ p_1 & p_0 & p_1 & \dots & p_N \\ p_2 & p_1 & p_0 & \dots & p_{N-1} \\ \vdots & \vdots & \vdots & \ddots & \vdots \\ 0 & p_N & p_{N-1} & \dots & p_0 \end{bmatrix}, \quad p_0 = -\frac{\Gamma(\alpha-1)}{\Gamma(\alpha/2+1)^2},$$
$$p_N = \left(1 - \frac{\alpha+1}{\alpha/2+N+1}\right)p_{N-1}, \tag{3.30}$$

in which $n = 1, 2, \dots, N$ is the index for the space discretization and N is the total number of space increments. Stability and convergence of the Finite Difference schemes are already verified elsewhere [Oldham and Spanier, 1974; Chaves, 1998; Çelik and Duman, 2012; Owolabi and Atangana, 2019].

3.3.2. *Solution of FRADE*

Solving the FRADE (3.24) for the transport rate C [Chaves, 1998; Benson *et al.*, 2000], neglecting solute transport by the pore fluid excess $\bar{Y}C$, requires the adoption of a proper numerical strategy; as stated previously, it is here assumed to refer to the Grünwald definition of the fractional derivative, Eq. (2.17), particularly referring to the shifted Grünwald–Letnikow formula [Oldham and Spanier, 1974]. Correspondingly, the final iterative system now becomes

$$(\mathbf{I} + \beta\mathbf{A} - \beta\mathbf{B})C^{t+1} = [\mathbf{I} - (1-\beta)\mathbf{A} + (1-\beta)\mathbf{B}]C^t + (\mathbf{F}^t + \beta\Delta\mathbf{F})\Delta t, \tag{3.31}$$

with

$$\mathbf{B} = \frac{\bar{K}}{2}\frac{\Delta t}{\Delta x^{\alpha}}[(1+\gamma)\mathbf{L} + (1-\gamma)\mathbf{L}^T], \quad \mathbf{L} = \begin{bmatrix} p_1 & p_0 & 0 & \cdots & 0 \\ p_2 & p_1 & p_0 & \cdots & 0 \\ p_3 & p_2 & p_1 & \cdots & 0 \\ \vdots & \vdots & \vdots & \ddots & \vdots \\ p_N & p_{N-1} & p_{N-2} & \cdots & p_0 \\ 0 & p_N & p_{N-1} & \cdots & p_1 \end{bmatrix},$$
$$p_N = \frac{\Gamma(N-\alpha)}{\Gamma(-\alpha)\Gamma(N+1)}, \tag{3.32}$$

with γ being a parameter accounting for the distribution probability of the relative weight of solute particle and $\mathbf{A}$ being a tridiagonal matrix related to the discretization of the advective term via the Lax–Wendroff scheme [Owolabi and Atangana,

2019],

$$\mathbf{A} = \begin{bmatrix} v^2 & -\frac{v(v-1)}{2} & 0 & \dots & 0 \\ -\frac{v(v+1)}{2} & v^2 & -\frac{v(v-1)}{2} & \dots & 0 \\ 0 & -\frac{v(v+1)}{2} & v^2 & \dots & 0 \\ \vdots & \vdots & \vdots & \ddots & -\frac{v(v-1)}{2} \\ 0 & 0 & 0 & -\frac{v(v+1)}{2} & v^2 \end{bmatrix},$$

$$v = V\frac{\Delta t}{\Delta x}, \tag{3.33}$$

where V is the average fluid velocity along the x-direction [substantially equivalent to $\bar{u}$ in Eq. (3.24)].

When accounting for pore fluid excess, the scheme proposed by Deng *et al.* [2006] has been followed, based on the split-operator method; particularly, it has been here assumed to solve the advection step via an explicit second-order midpoint method, the fractional diffusion/dispersion step via the aforementioned β-method, and the fluid excess step via the trapezoidal rule.

4. Numerical Examples

4.1. *Nonlinear FRDE*

In order to validate the fractional model, the numerical example of Çelik and Duman [2012] has been taken as the benchmark; correspondingly, the problem (3.26) has been subjected to the following homogeneous Dirichlet boundary conditions and initial conditions (for simplicity [Tasbozan *et al.*, 2013], a unit $\bar{K}$ has been assumed):

$$\begin{aligned} &C(0,t) = 0, && 0 < t \le T, \\ &C(1,t) = 0, && 0 < t \le T, \\ &C(x,0) = x^2(1-x)^2, && 0 < x < 1, \end{aligned} \tag{4.1}$$

and to the following forcing term:

$$\begin{aligned} f(x,t) = {} & (1+t)^{-1+\alpha}(-1+x)^2x^2 + \frac{1}{\Gamma(5-\alpha)}x^{-\alpha} + \left\{\left(\frac{1+t}{1-x}\right)^{\alpha}(-1+x)^2x^{\alpha}\right. \\ & \times [12x^2 - 6x\alpha + (-1+\alpha)\alpha] + (1+t)^{\alpha}x^2[12(-1+x)^2 + (-1+x)^2 \\ & \left. + (-7+6x)\alpha + \alpha^2]\right\}\sec\left(\frac{\pi\alpha}{2}\right). \end{aligned} \tag{4.2}$$

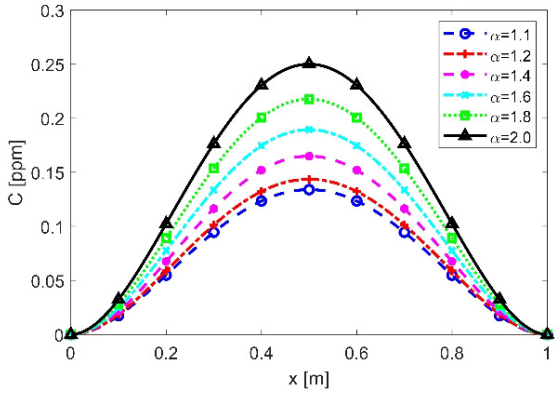

Fig. 6. Concentration profiles for the nonlinear 1D FRDE at $t = 1\,\mathrm{s}$.

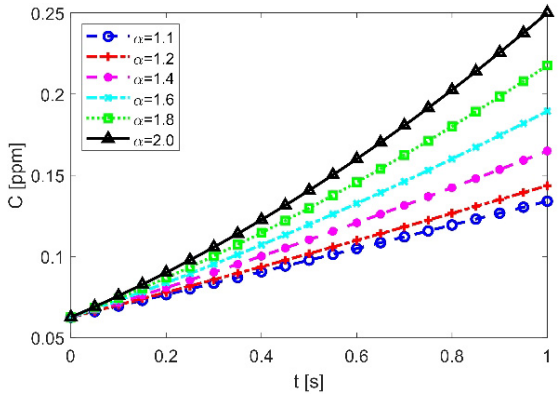

Fig. 7. Time evolution of concentration for the nonlinear 1D FRDE at $x = 0.5\,\mathrm{m}$.

The exact solution is given by

$$C(x,t) = (t+1)^{\alpha} x^2 (1-x)^2. \tag{4.3}$$

By adopting an explicit scheme ($\beta = 0$), a space increment $\Delta x = 0.01\,\mathrm{mm}$, and a time increment $\Delta t = 5 \cdot 10^{-5}\,\mathrm{s}$ (to respect the Courant–Friedrichs–Lewy stability condition), the results considering different values of the fractor α are plotted in Fig. 6 for $t = 1\,\mathrm{s}$ (final step), whereas at $x = 0.5\,\mathrm{m}$ in Fig. 7, with Figs. 8 and 9 reporting the comparisons with the analytical solution: particularly, a maximum error of 4.5% is evidenced at the model edges and of 0.03% in the middle, increasing and then stabilizing during the analysis due to the explicit structure of the temporal algorithm.

When approaching the classical dispersion ($\alpha = 2$), similarly to what was experienced in the case of linear FRDE, the concentration (alternatively, pressure) gradients change in space and time, so evidencing the effect of the fractional order; hence,

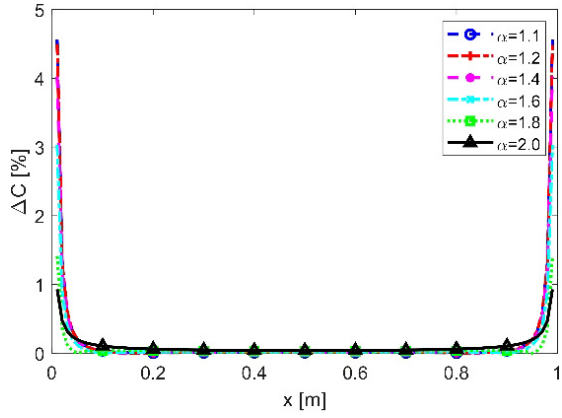

Fig. 8. Numerical–analytical percentage error for the nonlinear 1D FRDE at $t = 1\,\mathrm{s}$.

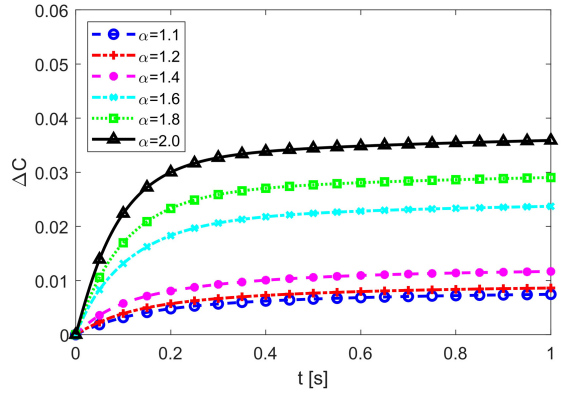

Fig. 9. Time evolution of percentage error for the nonlinear 1D FRDE at $x = 0.5\,\mathrm{m}$.

a non-Fickian mass transport shows an effect of retardation of the contaminant flow accounting for the medium heterogeneities.

4.2. *Nonlinear FRADE*

Problem (3.24), with negligible $\bar{Y}C$, has been subjected to the following initial and Dirichlet boundary conditions:

$$\begin{aligned} C(x,0) &= \begin{cases} 1 & x \leq 0 \\ 0 & x > 0 \end{cases}, \\ C(a,t) &= 1.0, \\ C(b,t) &= 0.0. \end{aligned} \tag{4.4}$$

Table 1. Material parameters for FRADE analysis.

Parameter	Value	Unit
a	-4	m
b	4	m
$\bar{K}$	0.2	m/s
v	0.5	m/s
N	160	—
T	200	—
t_{end}	1	s

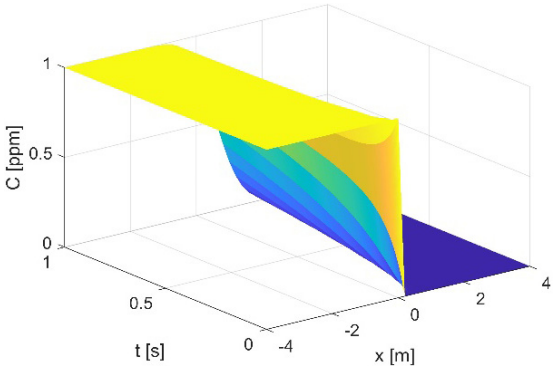

Fig. 10. Analytical solution for the standard AD problem [Sousa, 2009].

The adopted parameters are listed in Table 1, in which t_{end} is the final analysis time and T the total number of time steps; no forcing functions have been assumed, together with a zero probability term γ.

The analytical solution [Sousa, 2009] considering the classical Laplacian operator is given by (see Fig. 10)

$$C(x,t) = \frac{C(x,0)}{2}\left[1 - \text{erf}\left(\frac{x - Vt}{2\sqrt{\bar{K}t}}\right)\right]. \tag{4.5}$$

By adopting an explicit scheme, the results of Figs. 11 and 12 have been obtained, confirming [Fomin *et al.*, 2011] that the contaminant transport in the case of non-Fickian diffusion (correspondent to a fractal structure of the porous medium) in the direction of mainstream flow is predominantly determined by an advection mechanism, i.e., the second term in Eq. (3.26) drives the process and emphasizes the effect of the non-Gaussian tail [Deng *et al.*, 2004]; such an effect is particularly evident in zones with high concentration gradients.

When including $\bar{Y}C$, the following initial and Dirichlet boundary conditions have been used:

$$\begin{aligned} C(x,0) &= \frac{1}{\cosh(\rho x)}, \quad x \in [a,b], \\ C(a,t) &= C(b,t) = 0, \quad t > 0, \end{aligned} \tag{4.6}$$

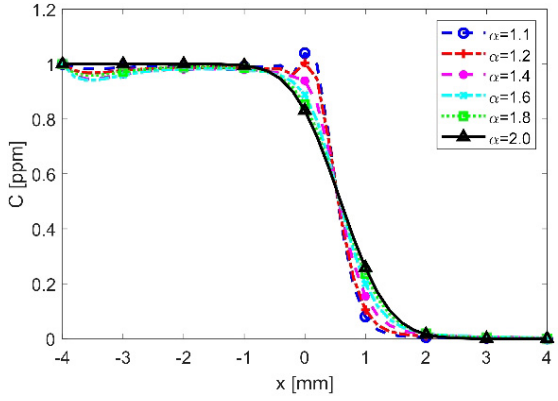

Fig. 11. Concentration profiles for the nonlinear 1D FRADE at $t = t_{\text{end}}$.

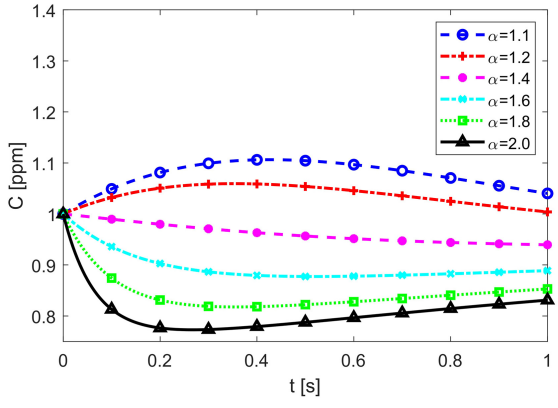

Fig. 12. Time evolution of concentration for the nonlinear 1D FRADE at $x = 0\,\text{m}$.

Table 2. Material parameters for the FRADE analysis with pore excess.

Parameter	Value	Unit
a	-10	m
b	10	m
ρ	0.5	m^{-1}
K	0.2	m/s
N	200	—
T	2,000	—
t_{end}	10	s

with the parameters being listed in Table 2 (with γ and the forcing function being zero); the main results are depicted in Figs. 13 and 14, again evidencing the contribution of the non-Gaussian tail even if reduced by the nonfractional overpressure term.

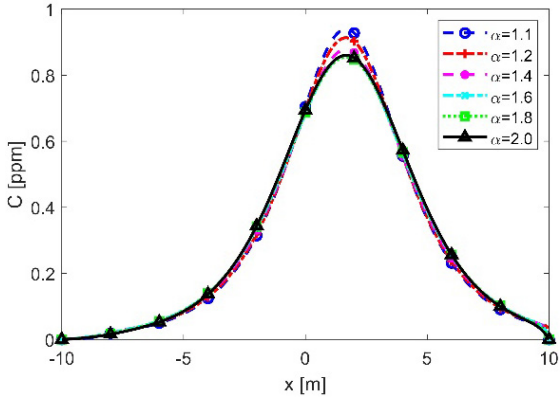

Fig. 13. Concentration profiles for the nonlinear 1D FRADE with pore excess at $t = t_{\text{end}}$.

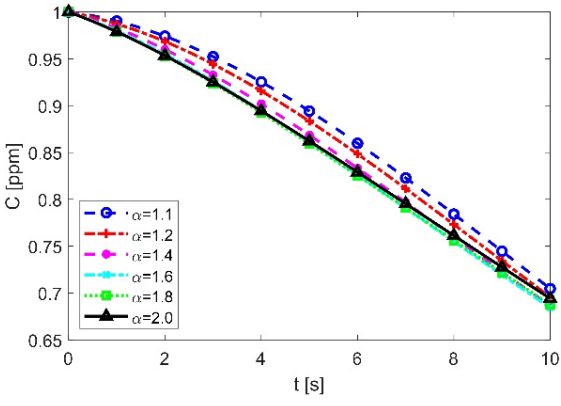

Fig. 14. Time evolution of concentration for the nonlinear 1D FRADE with pore excess at $x = 0\,\text{m}$.

5. Conclusions

A coupled three-dimensional fractional hydro-mechanical model in finite strains has been developed including solute transport and nonlinear fractional diffusion. A FRADE including overpressure effects has been particularly derived by extending the Fick's first law from isotropic media to heterogeneous media, so including heavy-tailed diffusion phenomena. By adopting the structure of the Riesz fractional derivative and choosing linear or nonlinear contribution of diffusion, the FRADE has been solved in 1D domains via Simpson's rule or a Finite Difference scheme based on the β-method. Particularly, a series of 1D Finite Difference analyses have been developed adopting the fractional-centered derivative scheme combined with the β-method, with the advective term treated via the Lax–Wendroff scheme. In the most general case of advection–dispersion phenomena including overpressure effects, the numerical algorithm has been enriched, so that the advection step has

been solved via an explicit second-order midpoint method, together with the β-method for the fractional diffusion/dispersion step and the trapezoidal rule for the fluid excess step. The algorithm, developed in MATLAB environment, has been validated against literature results, so confirming the correctness of the approach as well as allowing for appreciating the contribution from the tail part, increasing with high concentration/pressure gradients and with time. Particularly, it has been evidenced that the nonlocality of the fractional Laplacian affects the solution of water diffusion, influencing both the shape and the global diffusion velocity: the predicted fractional diffusion gradients appear lower than those for the standard diffusion independently of time, with the diffusion process appearing to be delayed. When considering anomalous solute diffusion, a non-Fickian mass transport shows the effect of retardation of the contaminant flow accounting for the medium heterogeneities; if advection is included, the effect of the non-Gaussian tail appears to be emphasized, apart from when the overpressure term is accounted for. The proposed fractional approach has been demonstrated to efficiently describe deviations from Darcy's law behavior together with, when contaminants are included, a positive reactivity disturbance phenomenon inducing longer simulation times.

Acknowledgments

Financial support from the Italian Ministry of Education, University, and Research (MIUR) in the framework of the Project PRIN2017 #2017HFPKZY is gratefully acknowledged.

References

Barkai, E., Metzler, R. and Klafter, J. [2000] "From continuous time random walks to the fractional Fokker–Planck equation," *Physical Review E* **61**(1), 132–138.

Barretta, R., de Sciarra, F. M., Pinnola, F. P. and Vaccaro, M. S. [2021] "On the nonlocal bending problem with fractional hereditariness," *Meccanica*, doi:10.1007/s11012-021-01366-8.

Benson, D. A., Wheatcraft, S. W. and Meerschaert, M. M. [2000] "The fractional-order governing equation of Levy motion," *Water Resources Research* **36**(6), 1413–1423.

Biot, M. A. [1941] "General theory of three-dimensional consolidation," *Journal of Applied Physics* **12**, 155–164.

Biot, M. A. [1956] "General solutions of the equations of elasticity and consolidation for a porous material," *Transactions of the ASME, Journal of Applied Mechanics* **23**, 91–96.

Blair, H. C., Schlesinger, P. H., Huang, C. L. H. and Zaidi, M. [2007] "Calcium signalling and calcium transport in bone disease," *Sub-cellular Biochemistry* **45**, 539–562.

Borja, R. I. [2004] "Cam-Clay plasticity: Part V: A mathematical framework for three-phase deformation and strain localization analyses of partially saturated porous media," *Computer Methods in Applied Mechanics and Engineering* **193**, 5301–5338.

Borja, R. I. [2013] *Plasticity — Modeling & Computation* (Springer-Verlag, Heidelberg).

Borja, R. I. and Alarcón, E. [1995] "A mathematical framework for finite strain elastoplastic consolidation — Part I: Balance laws, variational formulation, and linearization," *Computer Methods in Applied Mechanics and Engineering* **122**, 145–171.

Brusseau, M. L. [1994] "Transport of reactive contaminants in heterogeneous porous media," *Reviews of Geophysics* **32**, 285–313.

Caputo, M. [2000] "Models of flux in porous media with memory," *Water Resources Research* **36**(3), 693–705.

Carcione, J. M. and Gei, D. [2009] "Theory and numerical simulation of fluid-pressure diffusion in anisotropic porous media," *Geophysics* **74**(5), 31–39.

Çelik, C. and Duman, M. [2012] "Crank–Nicolson method for the fractional diffusion equation with the Riesz fractional derivative," *Journal of Computational Physics* **231**(4), 1743–1750.

Chaves, A. S. [1998] "A fractional diffusion equation to describe Levy flights," *Physics Letters A* **239**(1–2), 13–16.

Coussy, O. [2004] *Poromechanics* (John Wiley & Sons, New York, NY).

de Boer, R. [2005] *Trends in Continuum Mechanics of Porous Media: Theory and Applications of Transport in Porous Media* (Springer, New York, USA).

De Marchi, N., Salomoni, V. A. and Spiezia, N. [2019] "Effects of finite strains in fully coupled 3D geomechanical simulations," *International Journal of Geomechanics* **19**(4), 04019008.

Delgadino, M. G. and Smith, S. [2018] "Hölder estimates for fractional parabolic equations with critical divergence free drifts," *Annales de l'Institur Henri Poincaré C, Analyse non linéaire* **35**, 577–604.

Deng, Z. Q., Singh, V. P. and Bengtsson, L. [2004] "Numerical solution of fractional advection–dispersion equation," *Journal of Hydraulic Engineering* **130**(5), 422–431.

Deng, Z. Q., de Lima, J. L. M. P., de Lima, M. I. P. and Singh, V. P. [2006] "A fractional dispersion model for overland solute transport," *Water Resources Research* **42**, W03416.

de Pablo, A., Quiros, F., Rodriguez, A. and Vazquez, J. L. [2011] "A fractional porous medium equation," *Advances in Mathematics* **226**(2), 1378–1409.

del Teso, F. [2014] "Finite difference method for a fractional porous medium equation," *Calcolo* **51**, 615–638.

Detournay, E. and Cheng, A. H.-D. [1993] "Fundamentals of poroelasticity," in *Comprehensive Rock Engineering: Principles, Practice and Projects*, ed. C. Fairhurst, Vol. 2 (Pergamon Press, New York), pp. 113–171.

El-Amin, M. F., Radwan, A. G. and Sun, S. [2017] "Analytical solution for fractional derivative gas-flow equation in porous media," *Results in Physics* **7**, 2432–2438.

Elfeki, A. M. M., Uffink, G. J. M. and Barends, F. B. J. [1997] *Groundwater Contaminant Transport: Impact of Heterogeneous Characterization: A New View on Dispersion* (A.A.Balkema, Rotterdam, The Netherlands).

Fischer, H. B., List, E. J., Koh, R. C. Y., Imberger, J. and Brooks, N. H. [1979] *Mixing in Inland and Coastal Waters* (Elsevier, New York).

Fomin, S., Chugunov, V. and Hashida, T. [2010] "Application of fractional differential equations for modeling the anomalous diffusion of contaminant from fracture into porous rock with bordering alteration zone," *Transport of Porous Media* **81**, 187–205.

Fomin, S. A., Chugunov, V. A. and Hashida, T. [2011] "Non-Fickian mass transport in fractured porous media," *Advances in Water Resources* **34**, 205–214.

Goldsztein, G. H. [2008] "Solute transport in porous media: Media with capillaries as voids," *SIAM Journal of Applied Mathematics* **68**(5), 1203–1222.

Greco, A. and Iannizzotto, A. [2017] "Existence and convexity of solutions of the fractional heat equation," *Communications on Pure and Applied Analysis* **16**(6), 2201–2226.

Hilfer, R. and Anton, L. [1995] "Fractional master equations and fractal time random walks," *Physical Review E* **51**, R848–R851.

Holzapfel, G. A. [2000] *Nonlinear Solid Mechanics — A Continuum Approach for Engineering* (John Wiley & Sons, Chichester, UK).

Karrech, A., Regenauer-Lieb, K. and Poulet, T. [2011] "Frame indifferent elastoplasticity of frictional materials at finite strain," *International Journal of Solids and Structures* **48**(3–4), 397–407.

Karrech, A., Poulet, T. and Regenauer-Lieb, K. [2012] "Poromechanics of saturated media based on the logarithmic finite strain," *Mechanics of Materials* **51**, 118–136.

Knothe Tate, M. L. and Knothe, U. [2000] "An ex vivo model to study the transport processes fluid flow in loaded bone," *Journal of Biomechanics* **33**, 247–254.

Lewis, R. W. and Schrefler, B. A. [1998] *The Finite Element Method in the Static and Dynamic Deformation and Consolidation of Porous Media* (Wiley, Chichester).

Lewis, T. W., Pivonka, P. and Smith, D. W. [2009] "Theoretical investigation of the effects of consolidation on contaminant transport through clay barriers," *International Journal for Numerical and Analytical Methods in Geomechanics* **33**, 95–116.

Majorana, C. E. and Salomoni, V. A. [2004] "Parametric analyses of diffusion of activated sources in disposal forms," *Journal of Hazardous Materials* **113**, 45–56.

Majorana, C. E., Salomoni, V. A., Mazzucco, G. and Khoury, G. A. [2010] "An approach for modelling concrete spalling in finite strains," *Mathematics and Computers in Simulation* **80**(8), 1694–1712.

Mathur, S. and Jayawardena, L. P. [2008] "Thickness of compacted natural clay barriers in MSW landfills," *Practice Periodical of Hazardous, Toxic, and Radioactive Waste Management* **12**(1), 53–57.

McCutcheon, S. C. [1989] "Introduction to river and stream water quality modeling," in *Water Quality Modeling: Volume 1: Transport and Surface Exchange in Rivers* (CRC Press, Boca Raton), pp. 27–71.

Meerschaert, M. M., Benson, D. A. and Baumer, B. [1999] "Multidimensional advection and fractional dispersion," *Physical Review E* **59**(5), 5026–5028.

Meerschaert, M. M., Benson, D. A. and Scheffler, H. P. [2002] "Stochastic solution of space-time fractional diffusion equations," *Physical Review E* **65**, 041103(4).

Merryfield, K. G. [2009] Fourier Analysis, Course Notes, Department of Mathematics and Statistics, California State University, CA, http://web.csulb.edu/∼kmerry/.

Metzler, R. and Compte, A. [2000] "Generalized diffusion–advection schemes and dispersive sedimentation: A fractional approach," *The Journal of Physical Chemistry B* **104**, 3858–3865.

Neretnieks, I. [1980] "Diffusion in the rock matrix: An important factor in radionuclide retardation," *Journal of Geophysical Research, Solid Earth* **85**(B8), 4379–4397.

Nguyen, Q. H. and Vazquez, J. L. [2018] "Porous medium equation with nonlocal pressure in a bounded domain," *Communications in Partial Differential Equations* **43**(10), 1502–1539.

Oldham, K. B. and Spanier, J. [1974] *The Fractional Calculus* (Academic Press, New York, USA).

Owolabi, K. M. and Atangana, A. [2019] *Numerical Methods for Fractional Differentiation* (Springer, Singapore).

Peters, G. P. and Smith, D. W. [2002] "Solute transport through a deforming porous medium," *International Journal of Numerical and Analytical Methods in Geomechanics* **26**(7), 683–717.

Pinnola, F. P., Vaccaro, M. S., Barretta, R. and de Sciarra, F. M. [2021] "Random vibrations of stress-driven nonlocal beams with external damping," *Meccanica* **56**, 1329–1344.

Pomaro, B., Salomoni, V. A., Gramegna, F., Prete, G. and Majorana, C. E. [2011] "Radiation damage evaluation on concrete shielding for nuclear physics experiments," *Annals of Solid and Structural Mechanics* **2**, 123–142.

Salomoni, V. A. [2018] "A mathematical framework for modelling 3D coupled THM phenomena within saturated porous media undergoing finite strains," *Composites Part B: Engineering* **146**, 42–48.

Schrefler, B. A., Wang, X., Salomoni, V. and Zuccolo, G. [1999] "An efficient parallel algorithm for three-dimensional analysis of subsidence above gas reservoirs," *International Journal of Numerical Methods in Fluids* **31**(1), 247–260.

Schumer, S., Benson, D. A., Meerschaert, M. M. and Wheatcraft, S. W. [2001] "Eulerian derivation of the fractional advection–dispersion equation," *Journal of Contaminant Hydrology* **48**(1/2), 69–88.

Schumer, R., Benson, D. A., Meerschaert, M. M. and Baeumer, B. [2003] "Fractal mobile/immobile transport," *Water Resources Research* **39**(10), 1296.

Simo, J. C. and Hughes, T. J. R. [1998] *Computational Inelasticity* (Springer, New York).

Spiezia, N., Salomoni, V. A. and Majorana, C. E. [2016] "Plasticity and strain localization around a horizontal wellbore drilled through a porous rock formation," *International Journal of Plasticity* **78**, 114–144.

Stan, D., del Teso, F. and Vazquez, J. L. [2019] "Existence of weak solutions for a general porous medium equation with nonlocal pressure," *Archive for Rational Mechanics and Analysis* **233**, 451–496.

Sun, W. C. [2015] "A stabilized finite element formulation for monolithic thermo-hydro-mechanical simulations at finite strain," *International Journal of Numerical Methods in Engineering* **103**, 798–839.

Tasbozan, O., Esen, A., Yagmurlu, N. M. and Ucar, Y. [2013] "A numerical solution to fractional diffusion equation for force-free case," *Abstract and Applied Analysis* **2013**, 187383.

Vazquez, J. L. [2014] "Barenblatt solutions and asymptotic behaviour for a nonlinear fractional heat equation of porous medium type," *Journal of the European Mathematical Society* **16**(4), 769–803.

Vazquez, J. L. [2017] "The mathematical theories of diffusion: Nonlinear and fractional diffusion," in *Nonlocal and Nonlinear Diffusions and Interactions: New Methods and Directions*, eds. M. Bonforte and G. Grillo, Lecture Notes in Mathematics, Vol. 2186 (Springer, Cham), pp. 205–278.

Vazquez, J. L. [2018] "Asymptotic behaviour for the fractional heat equation in the Euclidean space," *Complex Variables and Elliptic Equations* **63**(7–8), 1216–1231.

Wang, L. [2018] "Solute transport in the bone lacunar-canalicular system (LCS)," *Current Osteoporosis Reports* **16**(1), 32–41.

Zhang, Y., Benson, D. A. and Reeves, D. M. [2009] "Time and space non-localities underlying fractional-derivative models: Distinction and literature review of field applications," *Advances in Water Resources* **32**, 561–581.

Zhang, H. J., Jeng, D. S., Barry, D. A., Seymour, B. R. and Li, L. [2013] "Solute transport in nearly saturated porous media under landfill clay liners: A finite deformation approach," *Journal of Hydrology* **479**, 189–199.

Zhou, H. W., Yang, S. and Zhang, S. Q. [2019] "Modeling non-Darcian flow and solute transport in porous media with the Caputo-Fabrizio derivative," *Applied Mathematical Modelling* **68**, 603–615.

Zou, L., Jing, L. and Cvetkovic, V. [2017] "Modeling of solute transport in a 3D rough-walled fracture-matrix system," *Transport in Porous Media* **116**, 1005–1029.